China Instrument and Control Society
Instrumentation
INSTRUMENTATION, Vol. 13, No. 2, June 2026
https://doi.org/10.15878/j.instr.202600345

Article

Design and Implementation of an Embedded Multi-Channel Data Acquisition System for Voltage, Current, Temperature, and Humidity Monitoring

Fangyuan Huang[1], Tianhu Wang[1*], Jungang Wang[2], Huijun Xia[3], Yihan Liu[3], Tailiang Yu[2]

[1] School of Electrical and Information Engineering, Jiangsu University of Technology, Changzhou, China

[2] Changzhou Metro Group Co., Ltd. Operation Branch, Changzhou, Jiangsu, 213000, China

[3] Jiangsu Rongxia Safety Technology Co., Ltd., Changzhou, Jiangsu, 213000, China

[*] Corresponding author email: tianhu2003@126.com

Abstract: To address the issue of insufficient channel capacity in single-signal acquisition systems at industrial sites, this paper designs a multi-channel data acquisition system based on embedded chips. The system adopts an architecture comprising an embedded controller and a host computer: the embedded controller handles signal conditioning, analog-to-digital conversion , filtering, and data transmission for multiple channels; while the host-computer software provides functions such as user login, data reception, real-time display, and storage. The modular architecture supports the conditioning and acquisition of voltage, current, temperature, and humidity signals. Test results showed that the relative errors of the voltage and current channels were below 1%, and that the system could acquire, transmit, display, and store the measured data.

Keywords: data acquisition; multi-channel; embedded systems; STM32; host-computer design

Citation: Fangyuan Huang, Tianhu Wang, Jungang Wang, Huijun Xia, Yihan Liu, Tailiang Yu."Design and Implementation of an Embedded Multi-Channel Data Acquisition System for Voltage, Current, Temperature, and Humidity Monitoring." Instrumentation 13, no.2 (June 2026). https://doi.org/10.15878/j.instr.202600345

1 Introduction

With the rapid development of industrial automation and Internet of Things (IoT) technologies, multi-channel data acquisition systems are playing an increasingly critical role in fields such as industrial monitoring, equipment diagnosis, and environmental sensing[1-3]. In complex industrial settings, there is a frequent need to synchronously acquire multiple analog signals, such as voltage, current, temperature, and humidity, placing high demands on the real-time capability, accuracy, and reliability of the data[4]. However, traditional single-channel or limited-channel acquisition devices struggle to meet the demand for parallel acquisition of multiple signals. Furthermore, they are often affected by issues like noise interference and channel crosstalk, which constrain the overall performance of monitoring systems.

In recent years, the continuous improvement in embedded processor performance and the widespread adoption of high-resolution ADCs have laid a hardware foundation for implementing multi-channel data acquisition systems[5-6]. Microcontrollers represented by the ARM Cortex-M series, such as STM32, have become a core choice for small to medium-sized acquisition systems due to their rich peripheral resources, low-power characteristics, and mature ecosystem[7-8]. Simultaneously, the combination of modular hardware design methods and configurable host-computer software has further enhanced system flexibility and scalability[9-10].

Despite ongoing improvements in hardware performance, the acquisition of multiple signal types in industrial environments still faces several challenges. On one hand, analog signals output from sensors exhibit

significant variations in amplitude and impedance, necessitating the design of universal and high-precision conditioning circuits to adapt them to the ADC input range[11]. On the other hand, interference factors such as electromagnetic noise and temperature drift in the field can easily degrade signal quality, requiring suppression at both the hardware filtering and software algorithm levels[12-13]. Additionally, the synchronous acquisition, real-time transmission, and reliable storage of multi-channel data remain common practical engineering difficulties[14].

To address the aforementioned requirements and challenges, this paper designs and implements a multi-channel data acquisition system based on the embedded STM32 platform. Its main innovations and contributions are as follows: First, at the hardware design level, a modular and expandable signal conditioning circuit architecture is proposed. Unlike traditional fixed-gain single conditioning circuits, it supports universal adaptation for voltage (0-10 V), current (0-1.5 A), and temperature-humidity signals. The use of analog switches for multiplexing significantly reduces the demand on MCU I/O resources. Second, at the communication protocol level, a custom frame structure (including header, data, and trailer) and a command interaction mechanism are designed. Compared to simple protocol-free serial communication, this enhances the reliability and anti-interference capability of data transmission. Third, at the system integration level, host-computer software based on LabVIEW is developed, implementing user authentication, real-time data display, waveform plotting, and automatic storage functions. This forms a complete "acquisition-transmission-display-storage" workflow, providing more comprehensive human-machine interaction and data management capabilities than commonly seen pure hardware systems.

Experimental results demonstrate that the relative error of the system in DC voltage and current signal acquisition is less than 1%. The temperature and humidity measurements effectively reflect environmental variations. The system shows clear advantages in terms of accuracy, reliability, and integration level compared to similar simplified acquisition solutions.

2 System Hardware Design

2.1 System Overall Architecture

The proposed embedded multi-channel data acquisition system comprises two main components: an embedded data-acquisition card and host-computer software. The embedded controller is built around an STM32F103ZET6 microcontroller (STMicroelectronics, Geneva, Switzerland) and includes peripheral signal-attenuation and filtering circuits for multi-channel signal acquisition and preprocessing. The embedded-controller firmware performs analog-to-digital conversion, digital signal reconstruction, mean filtering, and data packaging for transmission. The host-computer program provides user login, data reception, processing, display, and data-storage functions for real-time monitoring and recording [15]. As shown in Fig. 1, the system consists of three functional modules: the signal-conditioning circuits, the embedded controller, and the host computer. These modules implement the complete workflow from signal acquisition to data processing, visualization, and storage.

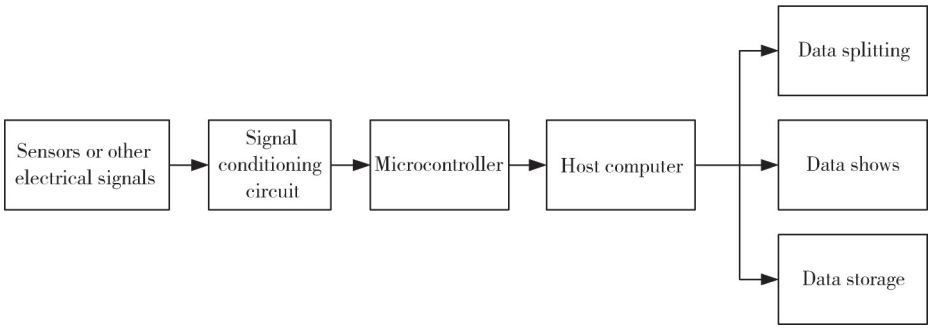

Fig.1 Overall Block Diagram

2.2 Signal Conditioning and Channel-Selection Circuit Design

This section describes the front-end circuits used to condition the measured signals before analog-to-digital conversion. The voltage and current conditioning circuits convert input ranges of 0-10 V and 0-1.5 A, respectively, into signals compatible with the 0-3.3 V ADC input range. The temperature and humidity acquisition module and the CD4051-based channel-selection circuit are also presented.

2.2.1 Voltage Signal Conditioning Circuit Design

Since the input voltage range of the microcontroller's built-in ADC module is determined by the reference voltages V_{REF+} and V_{REF-}, properly configuring the reference voltages is essential for ensuring effective signal acquisition. In this design, the V_{REF+} pin is externally connected to a 3.3 V reference voltage source, while the V_{REF-} pin is grounded. This configuration limits the ADC input range to 0-3.3 V, guaranteeing that the input signal remains within the detectable range at all times.

To accommodate the acquisition of wide-range 0-10 V voltage signals, a front-end voltage conditioning circuit was designed as shown in Fig. 2. This circuit is constructed based on an operational amplifier. The input signal is connected via port P1, undergoes voltage division through resistors and conditioning by the op-amp, and outputs a voltage signal meeting the ADC input requirements. The relationship between input and output is expressed by Equation (1):

$$V_+ = V_{in} * (\frac{R_2}{R_1 + R_2}) \quad (1)$$

The OP-07 operational amplifier is selected as the core component due to its low noise, high gain, and extremely low input offset voltage. In most applications, it requires no additional zero adjustment. Furthermore, the OP-07 maintains excellent linearity over a wide range, making it suitable for systems sensitive to nonlinear errors. In this circuit, the OP-07 forms a voltage follower, serving as a signal buffer for impedance matching[16,17]. Its primary function is to utilize its high input impedance and low output impedance characteristics to isolate the preceding voltage divider network from the subsequent filter and ADC, thereby preventing load effects from compromising measurement accuracy. Based on the operational amplifier's "virtual short and virtual open" principle, the relationship between its output and input is shown in Equation (2):

$$V_+ = V_- = V_{OUT} \quad (2)$$

This relationship ensures no attenuation of the signal during the buffering process. To further suppress high-frequency noise and prevent signal overshoot from damaging the ADC module, an RC low-pass filter circuit is connected at the signal output end, serving both filtering and overvoltage protection functions. Considering that the system primarily acquires slowly varying DC and low-frequency signals, the cut-off frequency is set to 160 Hz. This effectively filters out high-frequency interference while preserving the target signal. This frequency is jointly determined by resistor R_3 and capacitor C_2, as shown in Equation (3):

$$f_0 = \frac{1}{2\pi R_3 C_2} \quad (3)$$

Based on standard component values and considerations for circuit board layout, selecting R_3 = 10 kΩ and C_2 = 100 nF, substituting these values into the calculation yields a cutoff frequency of approximately 160 Hz, which meets the system's signal bandwidth requirements.

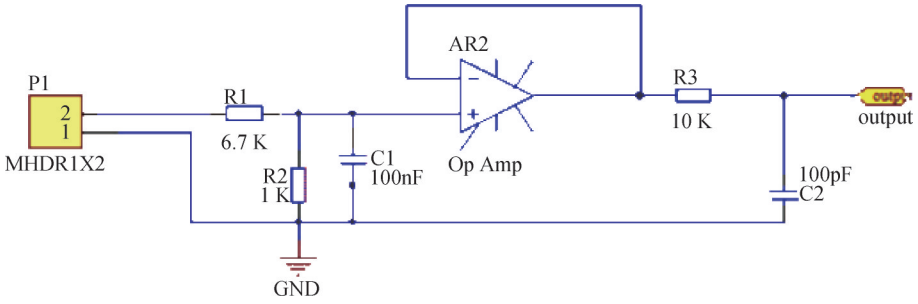

Fig.2 Front-End Voltage Signal Conditioning Circuit

2.2.2 Current Signal Conditioning Circuit Design

The current-signal conditioning circuit converts input currents of 0-1.5 A into voltage signals within the 0-3.3 V ADC input range. Its circuit structure is shown in Fig. 3. This circuit connects to the current signal under test via the P3 port. The current flows through a sampling resistor R_4 with a resistance of 0.1 Ω and an accuracy of ±1%, converting it into a corresponding voltage signal. According to Ohm's Law, this voltage value is proportional to the current, thereby enabling indirect measurement of the original current. This approach helps improve the overall measurement accuracy of the system.

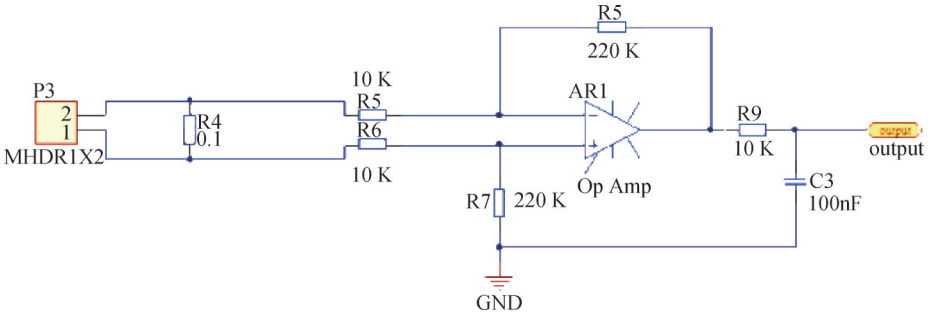

Fig.3 Front-End Current Signal Conditioning Circuit

During circuit operation, current flows through the sampling resistor R_4, generating corresponding minute voltage drops denoted as V_1 and V_2 (representing the potential across R_4). This differential voltage is amplified

and conditioned by the subsequent operational amplifier circuit, ultimately outputting a voltage signal V_{OUT} suitable for microcontroller acquisition. Based on the operational amplifier's "virtual short" and "virtual open" characteristics, the following set of equations can be established:

$$\begin{cases} \dfrac{V_2 - V_+}{R_6} = \dfrac{V_+}{R_7} \\ V_+ = V_- \\ \dfrac{V_2 - V}{R_5} = \dfrac{V_- - V_{OUT}}{R_8} \end{cases} \tag{4}$$

In order to amplify the small differential signal (0-0.15 V) across the sampling resistor to fit the optimal measurement range of the STM32's ADC (0-3.3 V), an amplification factor of approximately 22 is required. According to Equation (5):

$$V_{OUT} = \frac{R_8}{R_5} * (0 - 0.15) \tag{5}$$

To maintain V_{OUT} within the 0-3.3 V range, the resistance ratio between R_8 and R_5 must be appropriately set. This design selects R_8 = 220 kΩ and R_5 = 10 kΩ to meet the system's output range adaptation requirements.

2.2.3 Temperature and Humidity Acquisition Module

In natural environments, various physical quantities such as temperature, humidity, pressure, and gas concentration exist as continuous analog signals. Sensor technology emerged to effectively convert these signals into quantifiable electrical signals for acquisition. This design employs the DHT11 temperature and humidity sensor to collect and display real-time environmental temperature and humidity parameters.

The DHT11 sensor measures temperatures from 0-50 ℃ and relative humidity from 20-90%, offering advantages such as excellent stability, fast response speed, and low cost. It has been widely adopted in practical applications. This sensor incorporates pre-stored calibration coefficients, offering excellent sensitivity and linearity. It is suitable for temperature control and monitoring tasks in industrial environments. Its compact size and low power consumption meet the requirements of most application scenarios[18,19]. The physical diagram of the DHT11 module and its peripheral circuitry are shown in Fig. 4 and Fig. 5, respectively.

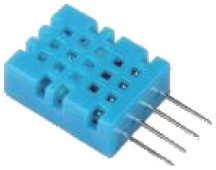

Fig.4 DHT11 Module

To integrate the acquisition of six analog signals—including two voltage signals, two current signals, and two sensor signals—while minimizing the number of

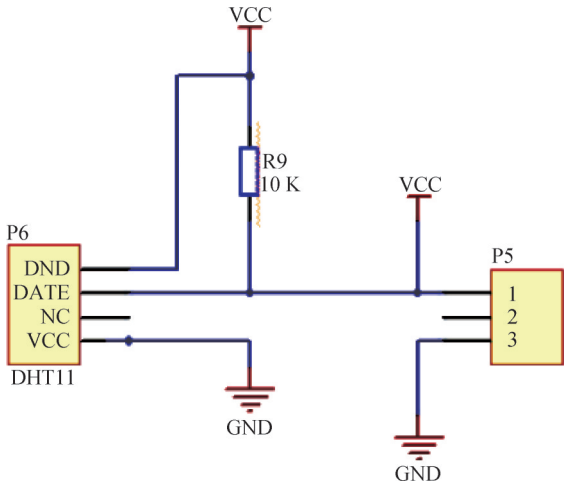

Fig.5 DHT11 Peripheral Circuit

microcontroller I/O ports occupied, this design employs a CD4051 analog switch for signal selection. The CD4051 is an 8-to-1 multiplexer where channel selection is controlled by a three-bit address code (A, B, C). When the INH pin is high, all channels are disabled[20]. Under single-supply operation, it can output signals with a peak-to-peak voltage of up to 15 V[21]. In this circuit, VDD = +5 V and VSS = VEE = 0 V. By applying 0-5 V digital control signals, it enables the selection and output of 0-3.3 V analog signals. All unused input ports are grounded to suppress interference. The physical diagram of the CD4051 is shown in Fig. 6.

Fig.6 CD4051 Physical Diagram

The operational amplifier selected for the signal conditioning circuit is the OP-07. This device features low offset voltage and high open-loop gain, making it particularly suitable for amplifying and processing weak signals[22,23]. All analog signals in the system are conditioned to the 0-3.3 V range. The OP-07 requires only ±5 V and 0 V power supplies to meet the design requirements. A physical diagram of the OP-07 is shown in Fig. 7.

Fig.7 Physical Diagram of 0P07

3 System Software Design

The system software comprises embedded-controller firmware and a host-computer interface. The embedded-controller firmware was developed using Keil µVision 5 (Arm Limited, Cambridge, UK) to implement signal acquisition, processing, and serial communication. The host-computer software was developed using LabVIEW 2024 (National Instruments Corporation, Austin, TX, USA) to provide data reception, real-time display, user interaction, and data-storage functions[24]. The following sections describe the implementation of the embedded-controller firmware and the host-computer software.

3.1 Embedded-Controller Firmware Design

Based on the hardware circuit design requirements, this section completes the embedded program development for the STM32F103ZET6 chip. The firmware was developed using Keil µVision 5 and downloaded to the STM32F103ZET6 microcontroller through an ST-Link programmer. Its code architecture is built upon standard library functions, incorporating the driver logic for the front-end signal conditioning circuit and the communication protocol with the host computer. The overall execution flow is illustrated in Fig. 8.

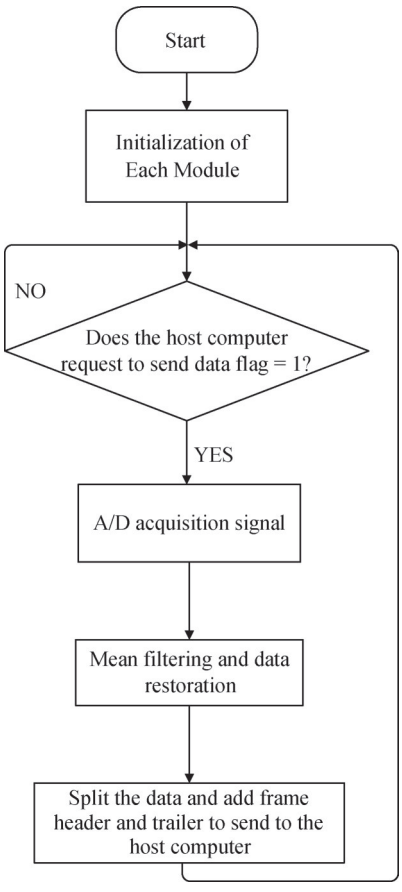

Fig.8 Embedded-controller Data Acquisition and Transmission Flowchart

The system initialization section configures the ADC, serial port, multiplexer control port, and DHT11 sensor. ADC initialization sets the input channel to PA1, operates at 12 MHz, and uses standalone mode with single conversion. Serial port initialization sets communication parameters and enables receive interrupts. Multiplexer control initialization configures PG0, PG2, and PG4 to push-pull output mode. DHT11 initialization configures the one-wire communication protocol based on its timing diagram.

The functional module implements core data processing and communication logic. The Task() function gates the corresponding channel of the CD4051, restores and applies mean filtering to the ADC-acquired data before storing it in the 24-byte array value, and triggers data transmission. USART1_IRQHandler() sets the transmission flag upon detecting the specific command sent by the host computer "11223344", initiating the data acquisition process; SendDebugData() appends the frame header 'AABBCCDD' and frame trailer "DDCCBBAA" to the data, forming a 32-byte data frame sent to the host computer.

After variable declarations, the main program sequentially calls initialization functions including Adc_Init(), USART1_Init(), Control_Init(), and DHT11_Init(). It then enters the main loop, continuously monitoring the serial send flag UsartSendFlag. When the host computer sends a request recognized by the interrupt service routine, this flag is set to "1". The main program then calls the Task() function to execute data acquisition and processing. The restored data is added to the frame structure and transmitted to the host computer. It is particularly important to note that to accurately restore the original physical quantity, the acquired data must be multiplied by the restoration factor m, i. e., $V_{actual} = m*V_{acquire}$, where $V_{acquire}$ is the signal after front-end conditioning[25]. The restoration factors for voltage and current signals are shown in Table 1.

Table 1 Restoration factor table

Signal Type	Reduction coefficient m
voltage signal (0-10 V)	3.075
current signal (0-1.5 A)	0.485

To quantitatively evaluate the system's performance and respond to the requirement for complexity analysis, the temporal characteristics and hardware resource utilization are analyzed.

Timing Analysis: The end-to-end latency is a key metric for real-time systems. The complete workflow from signal acquisition to data ready for transmission is depicted in Fig. 9. As illustrated, the process is deterministic and consists of sequential stages: the analog multiplexer (CD4051) switching time, the ADC conversion, digital processing (filtering and packaging), and finally UART serial transmission. The most significant contributor to the period is the serial

transmission. At 115, 200 baud, transmitting a 32-byte data frame requires approximately (32 × 10) / 115,200 ≈ 2.78 ms. The measured average period of the main acquisition task was 3.2 ± 0.2 ms, which aligns with the theoretical calculation and confirms the system's stable and predictable real-time performance.

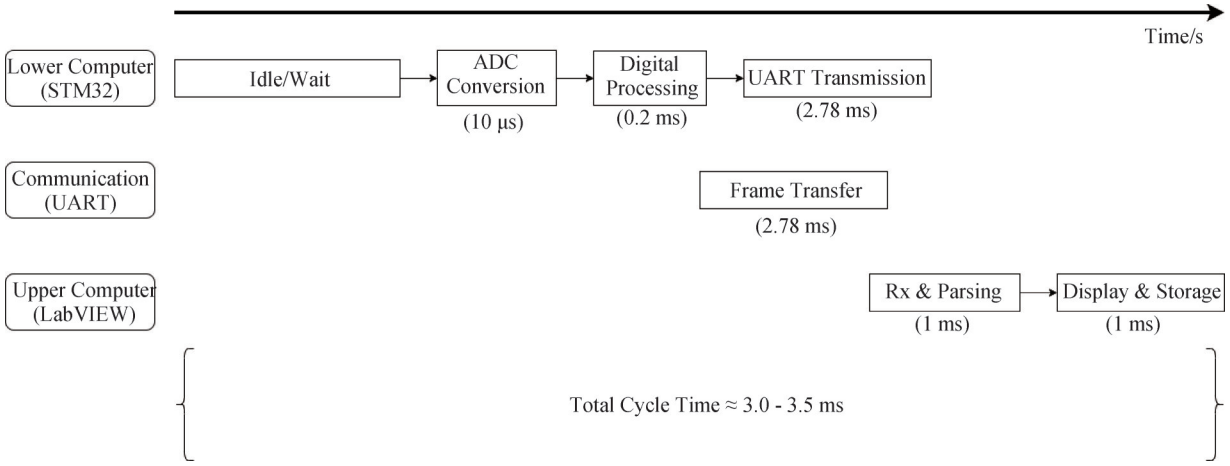

Fig.9 Timing Diagram for Data Acquisition and Transmission Cycle

Hardware Resource Utilization Analysis: Beyond timing, the optimization of hardware resource utilization represents a critical aspect of system-level complexity trade-off. The STM32F103ZET6 microcontroller typically has only 2-3 independent ADC peripherals. A conventional design to acquire six channels would require additional ADC chips, increasing system complexity and cost. The core innovation of this design lies in the channel multiplexing strategy using the CD4051 analog switch. This architecture allows six analog signals to be acquired by only one ADC peripheral, effectively saving five ADC hardware units. This strategic choice optimizes the use of constrained microcontroller resources and demonstrates a key design trade-off that prioritizes cost-effectiveness and reduced system complexity while fulfilling the multi-channel requirement.

3.2 Host-Computer Interface Design

The host-computer software was developed using LabVIEW 2024, featuring user login, digital signal waveform display, and data storage capabilities. The program comprises multiple modules including the login interface VI, serial communication VI, and account password management VI. Its core logic employs a simplified state machine architecture, encompassing six states: initialization, wait, send, get data, deal, and exit. Orderly transitions between these states form the complete system workflow[26,27]. The overall execution flow of the host-computer program is illustrated in Fig.10.

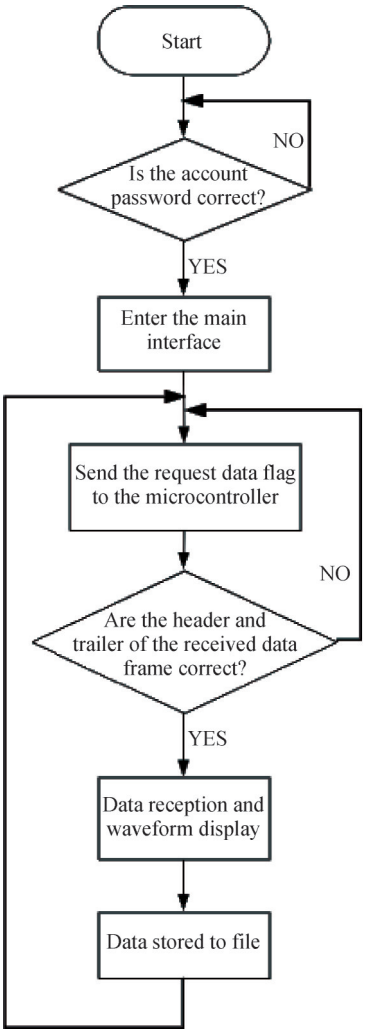

Fig.10 Flowchart of the host-computer program

The host-computer login interface employs an account-password verification mechanism. Preset credentials are stored in the "Account Password" VI. The system compares user input against the preset values: if either piece of information is incorrect, the front panel displays the prompt "Invalid account or password entered. Please re-enter. " Upon successful verification, the system enters the main interface of the multi-channel data acquisition system. The login interface is shown in Fig.11, and the block diagram of the Login Interface VI is shown in Fig.12.

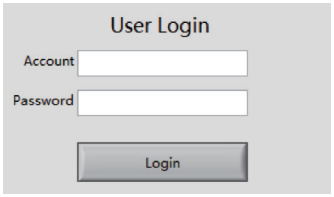

Fig.11 Login Interface

After the user clicks the "Open Serial Port" Boolean control on the front panel, the system transitions from the initialization state to the waiting state (wait) and initiates the serial port configuration process. This design employs USB-to-serial communication, which offers advantages of stable transmission and straightforward implementation. Within the LabVIEW environment, serial port parameters—including data bits, stop bits, baud rate, port number, and parity bit—are configured via VISA driver functions to complete serial port initialization. The system defines "11223344" as the request command sent by the host computer. The slave device only returns data after successfully verifying this instruction; otherwise, it ignores the request. After successful serial port initialization, the program enters the send state. The serial port initialization program and data request function are shown in Fig. 13 and Fig. 14, respectively.

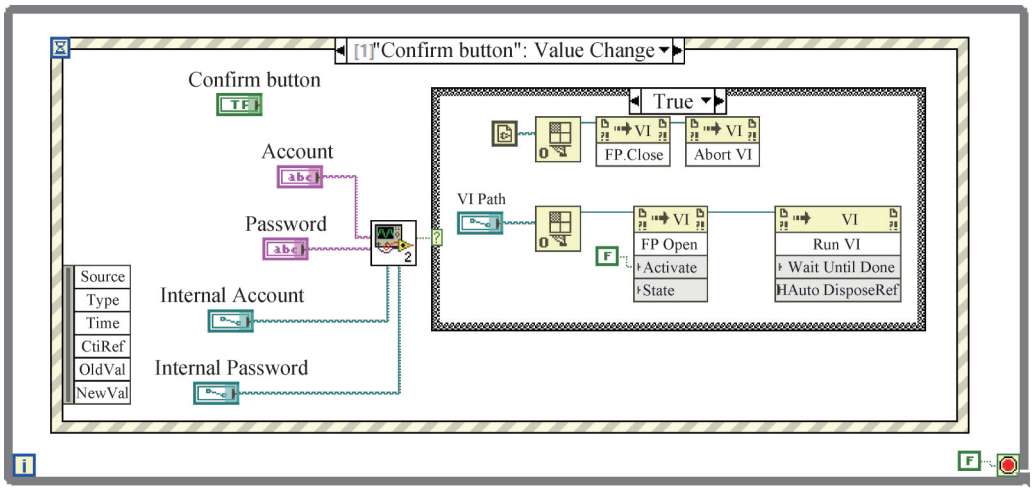

Fig.12 Block diagram of the Login Interface VI

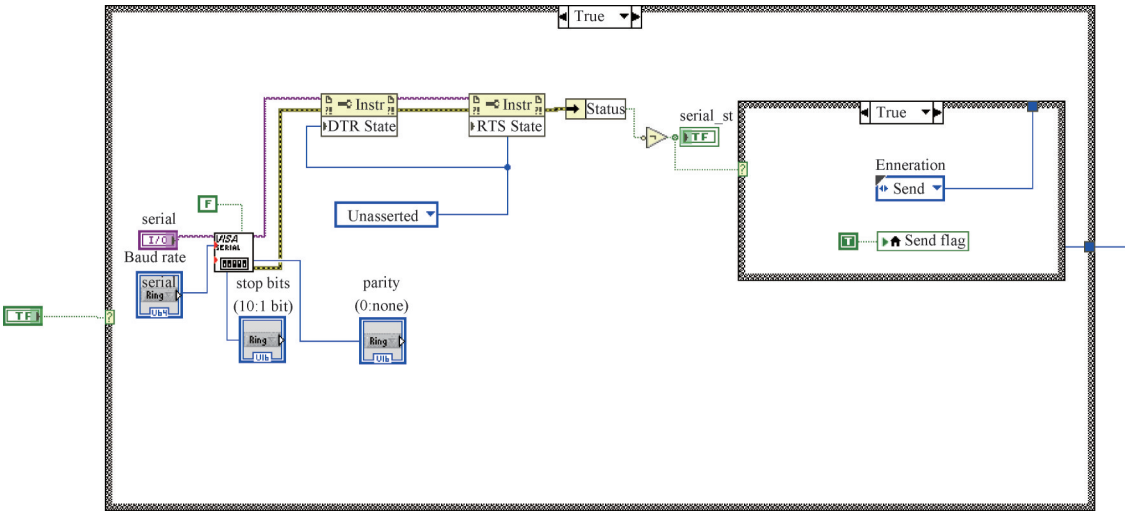

Fig.13 Serial Port Initialization Program

After the user completes the serial port parameter configuration, the program enters the send state and sends a data request to the embedded controller. It then transitions to the get data state. Upon receiving a valid command, the embedded controller returns 32 bytes of data via the serial port, comprising a 4-byte frame header, 24 bytes of six-channel acquisition data, and a 4-byte frame trailer. In the get data state, the host computer verifies the data length. If it is not 32 bytes, the data is discarded and the state is maintained. If the length requirement is met, the system transitions to the deal state to parse the frame structure and data content. The data request and byte count verification processes are illustrated in Fig. 14 and Fig. 15, respectively. In the deal state, the system first validates the frame header and trailer integrity. If validation fails, the data is discarded

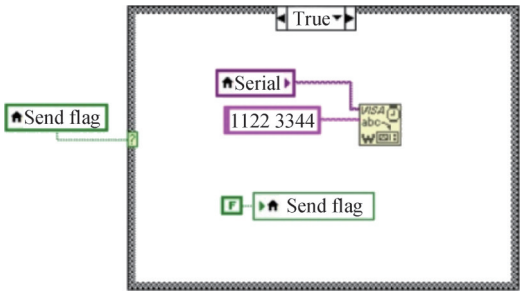

Fig.14 Data Request Program

and the system returns to wait state. Upon successful validation, the 24 bytes of valid data undergo parsing, segmentation, and format conversion to restore six floating-point values for real-time display. Upon completion, the data is simultaneously stored as a TXT file for subsequent analysis. The program ultimately returns to the wait state, cycling through the data acquisition process. The frame header/trailer determination and data processing logic are illustrated in Fig. 16.

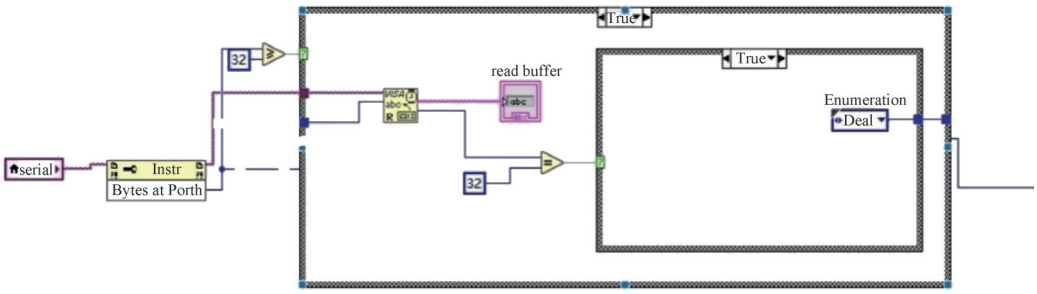

Fig.15 Byte Count Determination Program

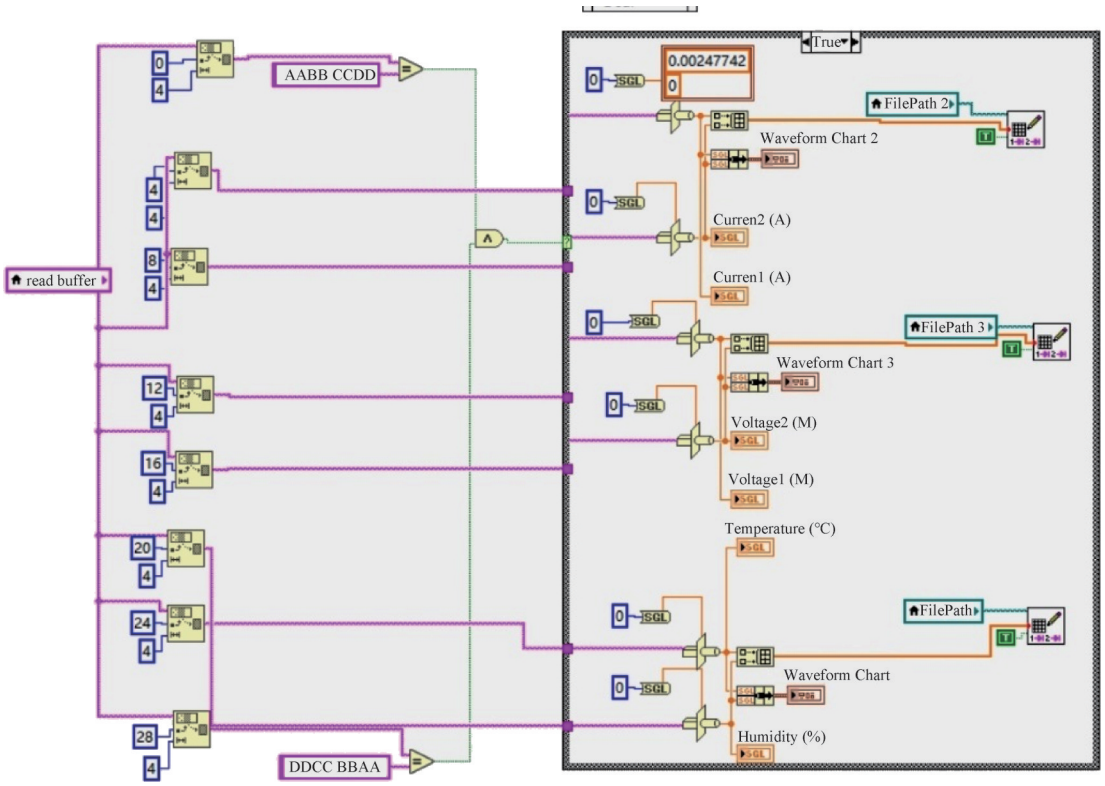

Fig.16 Frame validation and data-processing procedure

The system termination function is implemented via the exit state, which is triggered by the "Stop" Boolean control on the front panel. Upon user activation, the program closes the serial port connection, halts data reception, and resets all status flags. The system termination module program is illustrated in Fig. 17.

The system's main interface integrates core functions for data processing and serial port initialization. It displays collected data and corresponding waveform

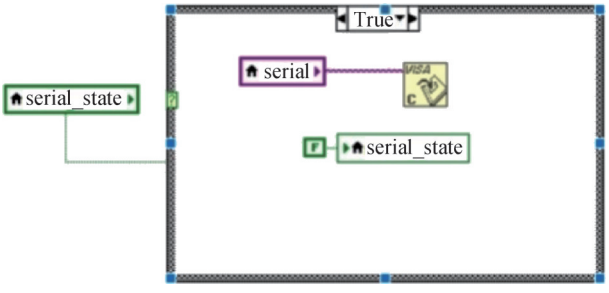

Fig.17 System Termination Procedure

charts in real time on the front panel. To enhance operational flexibility, parameters such as serial port number, stop bit, and parity bit are configured as adjustable options. Additionally, it features "Open Serial Port" and "Close Serial Port" Boolean controls. The interface provides controls for serial-port configuration and real-time displays of the acquired numerical values and waveforms, as shown in Fig. 18.

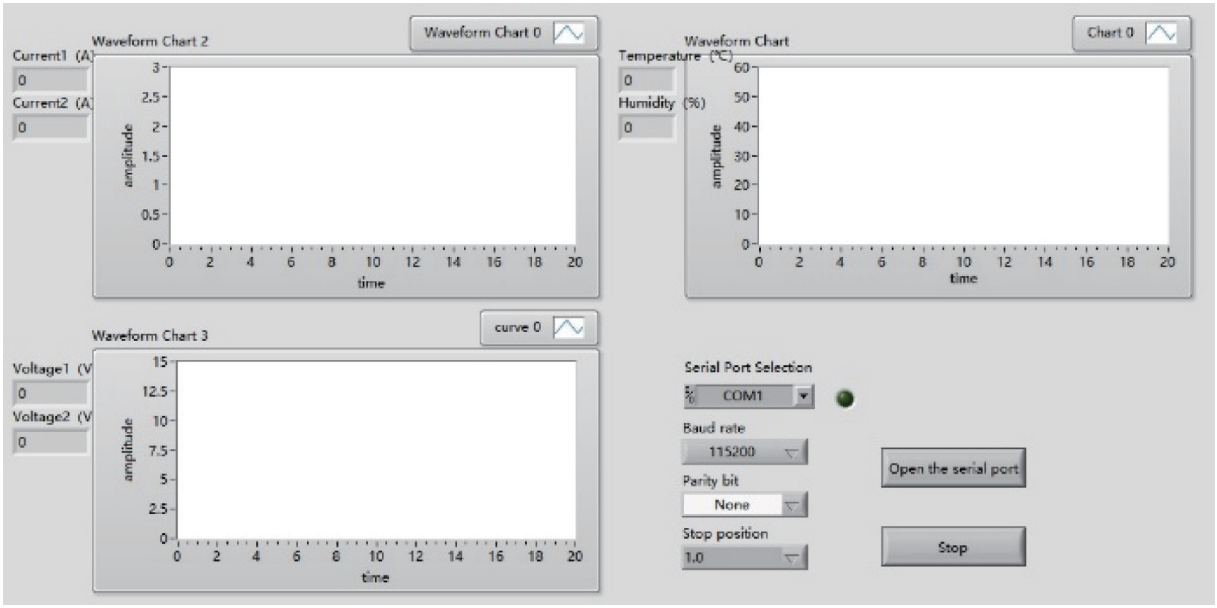

Fig.18 System Main Interface

4 Results and Discussion

This chapter covers system functional testing, encompassing embedded-controller hardware testing, host-computer functional testing, and measurement-error testing. System functional testing is an indispensable phase in system design and a critical safeguard for ensuring the system achieves its design objectives. After the initial completion of system design, functional testing must be conducted to identify design flaws and shortcomings, enabling timely corrections. Only through this process can an outstanding outcome that meets expectations be achieved.

4.1 Embedded-Controller Hardware Testing

Hardware testing is an indispensable critical step in the system design process, aimed at verifying product performance metrics and identifying potential issues and shortcomings. Through systematic testing and iterative problem resolution, design solutions can be continuously optimized, ultimately enhancing product performance. This hardware testing primarily focuses on the following aspects:

After confirming correct hardware connections, the voltage conditioning circuit, current conditioning circuit, and temperature/humidity module are connected to the microcontroller. The microcontroller is then connected to the host computer via an RS232-to-serial port module, establishing the communication foundation for subsequent functional testing. The physical connections for the conditioning circuit hardware are shown in Fig. 19.

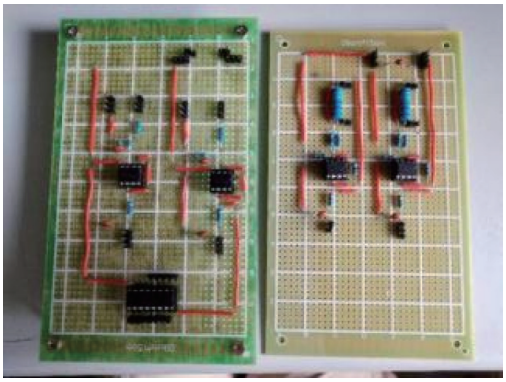

Fig.19 Hardware Schematic Diagram of the Conditioning Circuit

The test was conducted in a laboratory environment under normal temperature and humidity conditions. A commercially available MPS-3003L-3 DC regulated power supply was used to provide adjustable voltage and current signals for system testing. After confirming the hardware connections were correct, the system sequentially performed signal acquisition and communication tests on the voltage conditioning circuit, current conditioning circuit, and temperature-humidity module to verify the proper functionality of each channel[28,29].

4.2 Host-Computer Function Test

After successfully identifying the serial port, select the communication port (COM4) from the dropdown list, set the baud rate to 115,200, set parity to none, and set the stop bit to 1. Then click the Open Serial Port button. The

adjacent green indicator light signifies whether the serial port configuration initialization was successful. As shown in Fig. 20. The figure displays the acquired 3.3 V and 5 V signals, along with a temperature of 29 ℃ and humidity of 75%. This confirms normal communication between the host computer and the embedded controller and shows that the host-computer software can correctly display the acquired data.

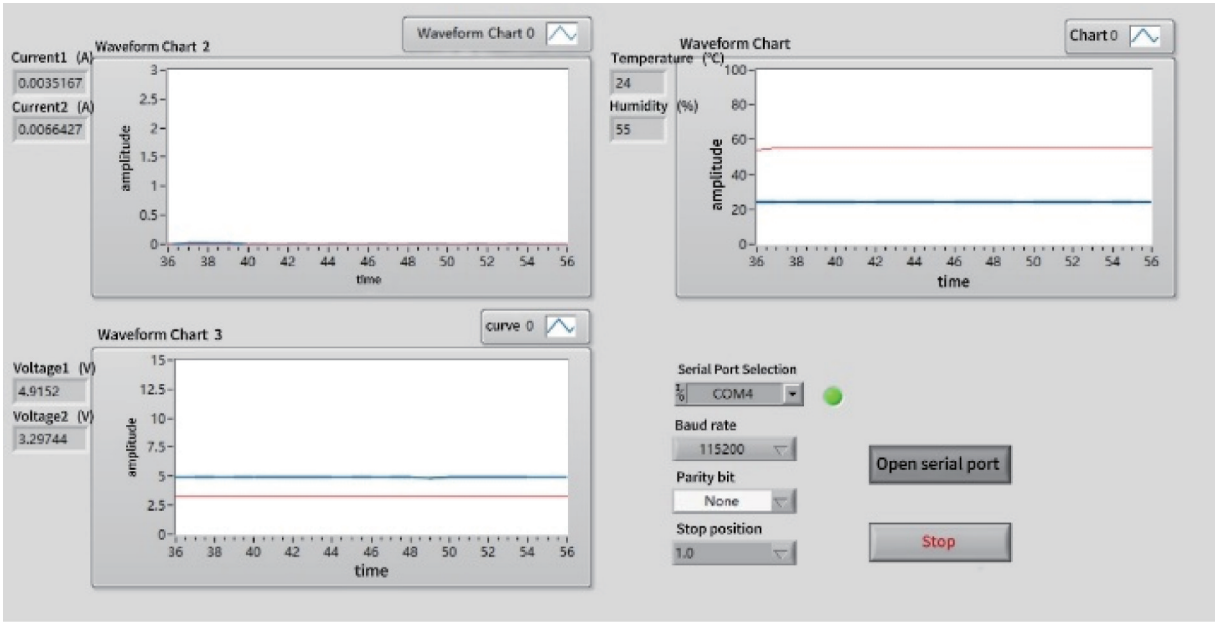

Fig.20 Main Interface Real-Time Display Chart

4.3 Data Error Testing

4.3.1 Sensor Signal Error Testing

Temperature and humidity data obtained from the temperature and humidity sensor are shown in Fig. 21(a) and (b):

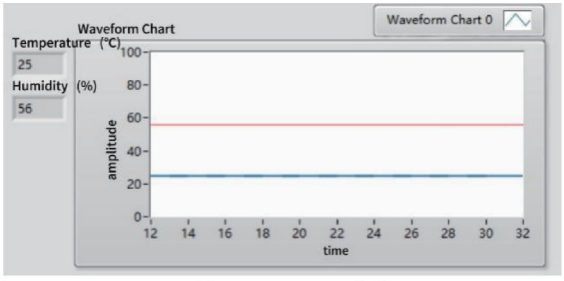

(a) temperature variation

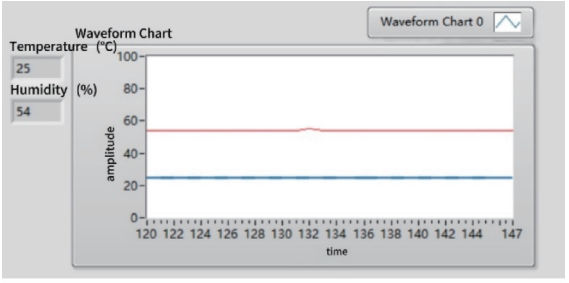

(b) relative-humidity variation

Fig.21 Environmental measurements:
(a) temperature variation; (b) relative-humidity variation

To eliminate interference during system startup, data recording must commence only after sensor readings stabilize to ensure accuracy. As shown in the graph, the temperature remains constant at 25° C, while humidity exhibits significant variation with an average of 55% RH. Although the data indicates limited precision in temperature and humidity measurements, overall readings align with normal values. This confirms that the temperature and humidity sensors meet design specifications for data acquisition, processing, and transmission.

4.3.2 Current and Voltage Signal Error Testing

The MPS-3003L-3 DC regulated power supply was used to provide reference voltage and current signals for the measurement-error tests. Data errors can be calculated based on the measured values from this system and the power supply's accurate values. Since errors are unavoidable, the microcontroller averages the data fifteen times before outputting the measured value. Subsequently, the average of four measured values is taken as the final result[30]. Finally, the relative error is calculated using Equations (6) and (7).

In Equation (6), V_T represents the average voltage measurement value, and V_0 denotes the standard voltage value.

$$\text{Relative Voltage Signal Error} = \frac{|V_T - V_0|}{V_0} \times 100\% \quad (6)$$

In equation (7), I_T represents the average value of the current measurement, and I_0 denotes the standard current value.

$$\text{Relative Current Signal Error} = \frac{|I_T - I_0|}{I_0} \times 100\% \quad (7)$$

Based on the above steps, the measurement tables for the two voltage signals and two current signals are shown in Tables 2 and 3. After multiple data acquisition measurements for each signal channel, the following conclusions can be drawn from the multiple data sets in these two tables: the relative errors of the voltage and current signals are small, generally maintained within 1%, but individual data values exhibit significant fluctuations. For instance, when collecting the 1A signal for Current 1 and the 1A signal for Current 2, the variation in the four measured values is greater compared to other signal measurements.

Table 2 Voltage Signal Recording Chart

Signal Source	Standard Voltage (V)	Measured Value 1	Measured Value 2	Measured Value 3	Measured Value 4	Signal Average	Relative Error (%)
Voltage 1	10	10.0145	10.1025	10.0623	10.1108	10.0580	0.58%
	5	5.1108	5.0378	5.0389	5.0246	5.0424	0.84%
	3.3	3.3201	3.3011	3.2936	3.3097	3.3049	0.14%
Voltage 2	10	9.9875	10.1385	10.0023	10.0148	10.0286	0.28%
	5	5.1024	5.0475	4.9251	4.9089	4.9967	0.06%
	3.3	3.3072	3.2901	3.3046	3.3075	3.3019	0.06%

Table 3 Current-signal Measurement Results

Signal Source	Standard Current (A)	Measured Value 1	Measured Value 2	Measured Value 3	Measured Value 4	Signal Average	Relative Error (%)
Current 1	1.5	1.492	1.5023	1.5036	1.4909	1.4972	0.18%
	1	1.0145	0.9932	1.0201	1.0114	1.0098	0.98%
	0.5	0.4982	0.5012	0.5031	0.4931	0.4989	0.22%
Current 2	1.5	1.5028	1.5029	1.5014	1.4965	1.5009	0.06%
	1	1.0098	1.0136	0.9874	1.0261	1.0092	0.92%
	0.5	0.5022	0.4967	0.4931	0.5061	0.4995	0.09%

Overall, the multi-channel data acquisition system designed in this paper can achieve real-time, approximate detection of temperature and humidity values in the environment. For the measurement of DC voltage and current signals, the relative error is smaller, maintaining below 1%, meeting the expected system specifications.

Across the test results, the relative errors of the voltage channels ranged from approximately 0.06% to 0.84%, while those of the current channels ranged from 0.06% to 0.98%. The host-computer software successfully received, parsed, displayed, and stored the transmitted measurement data during the functional tests.

4.4 System Performance Analysis and Discussion

Based on the test results presented above, the system has achieved its design objectives. Its innovative value is validated through the following aspects:

Verification of High-Precision Acquisition Capability: The relative measurement error for voltage and current signals remains consistently below 1%. This result directly validates the effectiveness of the modular conditioning circuit proposed in this paper in maintaining linearity and accuracy across a wide input range (0-10 V, 0-1.5 A), overcoming the poor adaptability of traditional single-purpose conditioning circuits.

Verification of System Reliability and Integration Level: The host-computer main interface stably receives and displays six channels of data in real-time, and the temperature and humidity variation curves are coherent and valid. This demonstrates the reliability of the complete "acquisition-transmission-display-storage" workflow. This reliability benefits from the data transmission integrity ensured by the custom communication protocol and the effective multi-task coordination supported by the integrated LabVIEW host-computer software.

Alignment with Engineering Requirements: The system successfully achieves synchronous acquisition, conditioning, and monitoring of multi-channel signals. Its error level and integrated design meet the core industrial requirements for accuracy, reliability, and real-time performance as stated in the introduction. Compared to simplified acquisition solutions that only provide raw data, this system offers a more complete solution.

To further contextualize the contributions and design

trade-offs of the proposed system, Table 4 compares its key characteristics with two representative alternative solutions: high-end commercial data acquisition cards and simple microcontroller-based polling solutions.

Table 4 Comparison with representative data acquisition approaches

Feature Dimension	This Work (STM32-Based Multiplexed System)	Commercial DAQ Card[31]	Basic MCU Polling[32]
Hardware Cost	Very Low (Core components < $10)	Very High (Hundreds to thousands of dollars)	Low
Channel Scalability	High (Easily expanded via analog multiplexers)	Fixed (Limited by purchased model)	Low (Limited by native ADC pins)
Sampling Synchronization	Quasi-simultaneous (High-speed multiplexing)	True Simultaneous (Independent ADCs)	Sequential (Polling introduces skew)
Development Complexity	Medium (Requires hardware design & embedded code)	Low (Mature drivers & software)	Low (Simple coding, limited features)
Core Advantage	Customizability, Cost-Effectiveness for dedicated applications	High precision, speed, and ease of use	Prototyping simplicity, low learning curve
Typical Application	Custom industrial monitoring, embedded integration	Laboratory research, high-fidelity measurement	Hobbyist projects, educational demos

As evidenced by the table, the proposed system does not seek to outperform commercial solutions in terms of raw sampling rate or synchronization accuracy. Instead, it identifies a niche in low-cost, customizable, and embedded industrial applications. The primary complexity optimization lies not in algorithmic breakthrough but in an efficient system-level architecture that balances cost, flexibility, and sufficient performance for targeted scenarios. The use of an analog multiplexer is a key factor enabling this trade-off, reducing peripheral requirements on the MCU.

5 Conclusion

This study developed an STM32F103ZET6-based multi-channel data acquisition system for voltage, current, temperature, and humidity monitoring. The relative errors of the tested voltage channels ranged from approximately 0.06% to 0.84%, while those of the current channels ranged from 0.06% to 0.98%. The average acquisition cycle was 3.2 ± 0.2 ms. Functional tests confirmed that the system could acquire, transmit, display, and store the measured data.

Although the prototype supports the acquisition of multiple signal types, further improvements are possible in channel capacity and communication methods. Future work will focus on expanding the number of acquisition channels and evaluating wireless communication methods, such as Bluetooth, for applications requiring remote monitoring.

Author Contribution:

Conceptualization, T. W.; methodology, F. H.; investigation, F.H.; data curation, F.H.; formal analysis, F. H.; validation, J. W., H. X., Y. L. and T. Y.; writing—original draft, F. H.; writing—review and editing, T. W.; supervision, T.W. All authors have read and agreed to the published version of the manuscript.

Acknowledgments:

The authors have no acknowledgments to declare.

Foundation Information:

This research was funded by Changzhou Technology Project (No. CZ20250010), Natural Science Foundation of Jiangsu Province (BK20150247).

Data Availability:

The authors declare that the main data supporting the findings of this study are available within the paper.

Conflicts of Interest:

The authors declare no competing interests.

Dates:

Received December 10, 2025; Accepted April 16, 2026; Published online July 10, 2026

References

[1] Zheng Y., Zhao J., & Tang Y. (**2022**). Design of multi-channel data acquisition system based on FPGA [J]. *International Journal of Frontiers in Engineering Technology*, 4, 26-29.

[2] Weng, Kangjing. (**2023**). Application of distributed multi-channel real-time data acquisition and display system in civil aviation test. In 2023 10th International Forum on Electrical Engineering and Automation (IFEEA). IEEE.

[3] Zhang, Yilun. (**2022**). Research on multi-channel data acquisition system of production index information based on genetic algorithm [J]. *International Journal of Information and Communication Technology*, 20(3), 245-257.

[4] Toscani, Andrea, et al. (**2023**). A novel scalable digital data

acquisition system for industrial condition monitoring [J]. *IEEE Transactions on Industrial Electronics*, 71(7), 7975-7985.

[5] Pavlović, Vukašin, et al. (**2022**). A Data Acquisition System for the Wire Tensioning System in the RoboShepherd [J]. *Innovative Mechanical Engineering*, 1(3), 21-28.

[6] Cherukat, Shoukath, et al. (**2024**). *Non-intrusive Remote Apiculture Monitoring System. In NIELIT's International Conference on Communication, Electronics and Digital Technologies* . Singapore: Springer Nature Singapore.

[7] Ünsalan, Cem, Gürhan, Hüseyin Deniz, & Yücel, Mehmet Erkin. (**2022**). Embedded System Design with ARM Cortex-M Microcontrollers: Applications with C, C++ and MicroPython. Cham: Springer. *ISBN* 978-3-030-88439-0. doi: 10.1007/978-3-030-88439-0.

[8] Shaker, Hesham H., et al. (**2023**). Development of low-cost digital gamma spectrometer using ARM Cortex-M Type Microcontroller Unit [J]. *Journal of Instrumentation*, 18(6), T06003.

[9] Ma, Yibo, et al. (**2018**). Research on hand-held dual motor driven harvester for tree fruit [J]. *IFAC-PapersOnLine*, 51 (17), 268-273.

[10] Yang, Mengke, et al. (**2023**). *Design and Experimental Study of An Intelligent Soft Crawling Robot for Environmental Interactions. In International Conference on Intelligent Robotics and Applications*. Singapore: Springer Nature Singapore.

[11] Lei, Yang. (**2023**). Array Sensor Output Signal Detection System Signal Conditioning Circuit Design [J]. *Journal of Physics: Conference Series*, 2452(1).

[12] Nikitin, Alexei V., & Davidchack, Ruslan L. (**2018**). Analog-domain mitigation of outlier noise in the process of analog-to-digital conversion. In 2018 IEEE International Conference on Communications (ICC). IEEE.

[13] Wang, Fengjuan, et al. (**2023**). A compact sixth-order common-mode noise suppression filter based on 3-D integration technology [J]. *IEEE Transactions on Components* , Packaging and Manufacturing Technology, 13 (4), 502-510.

[14] Huang, Wuhuang, et al. (**2023**). Design of 16-channel high-speed synchronous data acquisition system. In 2023 IEEE AUTOTESTCON. IEEE.

[15] Ehsani, Behzad. (**2016**). Data Acquisition Using LabVIEW. *Packt Publishing Ltd* .

[16] Xiao Yongfu, Zhang Hao, & Zou Hao. (**2020**). Design of a Quad-Channel Analog Data Acquisition System Based on FPGA [J]. *Open Access Library Journal* , 7(12), 1-6.

[17] Manivannan M., & Kumaresan N. (**2011**). *Design of on-line interactive data acquisition and control system for embedded real-time applications* . In 2011 International Conference on Emerging Trends in Electrical and Computer Technology. IEEE.

[18] L. V. Grunskaya, A. N. Zolotov, & A. S. Bushuyev. (**2019**). Universal data acquisition system for monitoring environmental characteristics [J]. *IOP Conference Series: Materials Science and Engineering*, 698(4), 27-33.

[19] Puchianu D. C. (**2021**). Amplifier circuit with LM324 operational amplifier: Analytical calculation, Octave and OrCAD LITE simulation [J]. *The Scientific Bulletin of Electrical Engineering Faculty*, 21(2), 13-16.

[20] Helen-Maria Dounavi, Yiorgos Sfikas, & Yiorgos Tsiatouhas. (**2019**). Periodic Monitoring of BTI Induced Aging in SRAM Sense Amplifiers [J]. *IEEE Transactions on Device and Materials Reliability*, 19(1), 64-72.

[21] Ramesh Chandra Poonia & Vaibhav Bhatnagar. (**2022**). Design of decision support system to identify crop water need [J]. *Journal of Ambient Intelligence and Humanized Computing* , 1-8.

[22] Yusuf Panessai Ismail Ismail, bin Lakulu Muhammad Modi, Subramaniam Siva Kumar A/L, Saad Ahmad Fadli, Damanhuri Muhd Ibrahim Muhamad, & Yusuf Nur Iksan. (**2019**). Developing a Prototype for Sun Tracker System Based on IoT: Controlled by Mobile App and Online Database Monitoring [J]. *American Journal of Applied Sciences*, 16(1), 11-25.

[23] Jadhav, Suraj S., et al. (**2025**). *Design and Implementation of a Cybersecurity-Enhanced Four-Channel EEG Monitoring System Using Eight Electrodes. In International Conference on Security and Privacy* . Cham: Springer Nature Switzerland.

[24] Asadi, Farzin. (**2023**). Multiplexer and De-multiplexer. In Digital Circuits Laboratory Manual, pp. 81-104. Cham: Springer Nature Switzerland.

[25] Choudhury, Pradyumna Kumar, & Baruah, Debendra Chandra. (**2024**). Microcontroller-based integrated data logging system for solar air heater performance assessment [J]. *Energy Sources, Part A: Recovery, Utilization, and Environmental Effects* , 46(1), 11435-11451.

[26] Xiaozheng Wang, Yahui Wang, & Da Zhao. (**2022**). Research on Data Acquisition System of Pipeline Snake Robot. In 2022 34th Chinese Control and Decision Conference (CCDC). IEEE.

[27] Wang, Xingju. (**2014**). Design of temperature measurement and data acquisition system based on virtual instrument LabVIEW [J]. *TELKOMNIKA Indonesian Journal of Electrical Engineering*, 12(8), 6027-6035.

[28] Huber, Patrick, Göhner, Ulrich, Trapp, Mario, Zender, Jonathan, & Lichtenberg, Rabea. (**2025**). Comprehensive Analysis of Neural Network Inference on Embedded Systems: Response Time, Calibration, and Model Optimisation [J]. *Sensors*, 25(15), 4769. doi:10.3390/s25154769.

[29] Zhang, Xiaodan, et al. (**2024**). A High-Speed Data Acquisition and Control System Based on LabVIEW for Long-Pulse Experiments. In 2024 6th International Conference on Communications, Information System and Computer Engineering (CISCE). IEEE.

[30] Li, Jiaying, & Wang, Yonglong. (**2024**). A High-Precision Data Acquisition System Designed by Using AD7606 and LabVIEW. In 2024 3rd International Symposium on Semiconductor and Electronic Technology (ISSET). IEEE.

[31] Song, Yuge, et al. (**2023**). Fast calibration with raw data verification for current measurement of dual-PMSM drives [J]. *IEEE Transactions on Industrial Electronics*, 71(7), 6875-6885.

[32] Kobelev D. I., & Jordan V. I. (**2021**). *Application of a precision programmable DC power supply for spectrometer calibration*[J]. Journal of Physics: Conference Series, 1843(1).